Applied Mathematical Modelling 38 (2014) 4778–4795

Contents lists available at ScienceDirect

Applied Mathematical Modelling

journal homepage: www.elsevier.com/locate/apm

Fundamental solutions of uniform loads over triangular elements in a three-dimensional piezoelectric medium

QiaoYun Zhang [a], CuiYing Fan [b,d], MingHao Zhao [a,b,d], Ernian Pan [b,c,*]

[a] School of Mechanics and Engineering Science, Zhengzhou University, Zhengzhou, Henan Province 450001, China
[b] School of Mechanical Engineering, Zhengzhou University, Zhengzhou, Henan Province 450001, China
[c] Department of Civil Engineering, University of Akron, Akron, OH 44325, USA
[d] Henan Key Engineering Laboratory for Anti-fatigue Manufacturing Technology, Zhengzhou, Henan Province 450001, China

ARTICLE INFO

Article history:
Received 13 February 2013
Received in revised form 2 January 2014
Accepted 18 March 2014
Available online 1 April 2014

Keywords:
Transverse isotropy
Piezoelectricity
Three-dimensional space
Triangular load
Fundamental solution

ABSTRACT

In this paper, fundamental solutions of uniform loads over triangular elements in an infinite transversely isotropic piezoelectric three-dimensional space are derived. The triangle element can be parallel or vertical to the plane of isotropy and the uniform load can be mechanical and electric types, oriented in an arbitrary orientation. The solutions are expressed simply as a linear combination of three kinds of elementary functions – linear, trigonometric and logarithm functions. Three methods of superposition are employed to verify the obtained fundamental solutions. Numerical examples are also presented for the extended displacements and stresses induced by both mechanical and electric loads on the vertical and horizontal triangles.

© 2014 Elsevier Inc. All rights reserved.

1. Introduction

Green's functions or fundamental solutions are very useful in constructing analytical solutions and further play important roles in boundary integral equation method and boundary element method. Research on fundamental solutions of conventional elastic material problems and structures has been attracting much attention [1–6]. With the rapid development of modern technology and owing to the coupling effect between the mechanical and electric properties, piezoelectric materials are now used in many important technologic fields. The extensive study of mechanical–electric behaviors for this kind of materials and structures under the combined mechanical–electric loads has been carried out. For two-dimensional (2D) piezoelectric media, Pan [7] derived the Green's functions in the full, half, and bimaterial planes. For 3D piezoelectric media, Ding et al. [8], Dunn and Wienecke [9], and Chen et al. [10] obtained the Green's functions in the full, half, and bimaterial spaces of transverse isotropy. While Pan and Tonon [11] derived the Green's functions in a general anisotropic piezoelectric infinite space, Gao and Wang [12] obtained the Green's functions in a bimaterial piezoelectric plane with a permeable interfacial crack. Ding et al. [13] summarized the Green's function solutions for both 2D and 3D transversely isotropic piezoelectric materials. For fracture mechanic of piezoelectric media, Zhao et al. [14] derived the extended displacement discontinuity fundamental solutions for 3D piezoelectric media, where the extended displacement discontinuities include the elastic displacement discontinuities and the electric potential discontinuity.

* Corresponding author at: Department of Civil Engineering, University of Akron, Akron, OH 44325, USA. Tel.: +1 330 972 6739.
E-mail address: pan2@uakron.edu (E. Pan).

http://dx.doi.org/10.1016/j.apm.2014.03.026
0307-904X/© 2014 Elsevier Inc. All rights reserved.

In engineering applications, a solid could be subjected to an arbitrary load over an arbitrarily shaped area. Thus, solutions for uniformly distributed loads over a given area in the shape of circle, rectangle or triangle are particularly appealing since these solutions can be applied as the fundamental solutions to the general load case. For crack analysis, Crouch [1] presented a 2D fundamental solution for conventional elastic materials, where the uniform displacement discontinuities are applied on a line element. Fan et al. [15] and Zhao et al. [16] obtained the extended Crouch fundamental solutions of linear elements in piezoelectric media and studied the finite and infinite, linear and nonlinear fracture problems in piezoelectric media. Zhao et al. [17,18] also studied the fundamental solutions of rectangular element in the corresponding 3D media.

For fundamental solutions induced by forces, the polynomial load problem over a triangular area on the surface of an isotropic elastic half space was solved by Svec and Gladwell [19]. A linear normal load over a triangular and rectangular area on the isotropic elastic half space was attacked, respectively, by Kalker and van Randen [20] and Dydo and Busby [21]. Wang and Liao [22] proposed the elastic solution for arbitrarily shaped and arbitrarily distributed loads in a transversely isotropic half space using the triangulating technique. The surface deflection due to constant and linear (normal and tangential) loads over a triangular area on the surface of the isotropic elastic half space was solved by Li and Berger [23]. Recently Xiao and Yue [24] solved the elastic fields in two joined transversely isotropic media of infinite extent due to rectangular loading.

So far, however, there is no exact closed-form solution for the displacement and stress fields in a 3D piezoelectric medium due to force loads over a circular, rectangular or triangular element, even for the common symmetric structures of transverse isotropy [25]. Thus, in this paper, we derive the fundamental solutions in a transversely isotropic piezoelectric full space due to uniformly distributed loads over a triangle by integrating the corresponding point-force Green's functions. The element can be a triangle which is either parallel or vertical to the material plane of isotropy, with the uniform load being oriented arbitrarily, including also the electric load. The correctness of the exact closed-form solutions is further validated by three different methods of superposition discussed in the paper. Numerical results are presented on the distribution of the electric potential and electric field as well as the displacement and stress fields.

2. Basic equations

We consider a linear and transversely isotropic piezoelectric infinite space with its isotropic plane parallel to the *oxy* plane in the Cartesian *oxyz* ($ox_1x_2x_3$) system. The poling direction is along the positive *z*-axis. In this paper, summation over repeated subscripts is assumed from 1 to 3 (1 to 4) for lowercase (uppercase) letters. We first define the following extended quantities:

Extended displacements: u_I (u_i; $u_4 = \phi$), where u_i are the elastic displacements and ϕ the electric potential;
Extended stresses: σ_{iJ} (σ_{ij}; $\sigma_{i4} = D_i$), where σ_{ij} are the elastic stresses and D_i the electric displacements;
Extended tractions with outward normal $\boldsymbol{n}$: P_I ($P_i = \sigma_{ij}n_j$; $P_4 = \omega \equiv D_jn_j$), where P_i are the elastic tractions and ω is the boundary value of the normal electric displacement.

We now assume that there is a distributed extended (traction) load $P_I(\boldsymbol{x})$ over an internal surface $S(\boldsymbol{x})$ with outward normal $\boldsymbol{n}$ in the space. Then, the induced extended displacements u_J and stresses σ_{iJ} can be obtained by surface integrals

$$u_J(\boldsymbol{x}^f) = \int_S P_K(\boldsymbol{x}) u^*_{JK}(\boldsymbol{x}^f;\boldsymbol{x}) dS(\boldsymbol{x}), \tag{1}$$

$$\sigma_{iJ}(\boldsymbol{x}^f) = \int_S P_K(\boldsymbol{x}) \sigma^*_{iJK}(\boldsymbol{x}^f;\boldsymbol{x}) dS(\boldsymbol{x}), \tag{2}$$

where $u^*_{JK}(\boldsymbol{x}^f;\boldsymbol{x})$ are the extended displacement in *J*-direction at field point $\boldsymbol{x}^f$ due to a point load in *K*-direction at source point $\boldsymbol{x}$, and $\sigma^*_{iJK}(\boldsymbol{x}^f;\boldsymbol{x})$ are the extended stresses with components *iJ* at field point $\boldsymbol{x}^f$ due to a point load in *K*-direction at source point $\boldsymbol{x}$. The detailed expressions of these Green's function solutions can be found in Zhao et al. [18,26].

3. Fundamental solutions for triangular elements in the isotropic plane (i.e., *oxy* plane)

We first assume that the internal surface *S* is made of a triangle *ABC* in the isotropic *oxy* plane over which the uniform load P_I is applied. We denote by $A(x_1, y_1)$, $B(x_2, y_2)$ and $C(x_3, y_3)$, the three vertices of the triangle, as shown in Fig. 1. Then the three lines or sides of the triangle (*AB*, *BC*, *CA*) defined by $LN_1(x)$, $LN_2(x)$ and $LN_3(x)$ can be expressed as

$$\begin{aligned} LN_1(x) &= y_1 + \frac{y_2 - y_1}{x_2 - x_1}(x - x_1), \\ LN_2(x) &= y_2 + \frac{y_2 - y_3}{x_2 - x_3}(x - x_2), \\ LN_3(x) &= y_3 + \frac{y_3 - y_1}{x_3 - x_1}(x - x_3). \end{aligned} \tag{3}$$

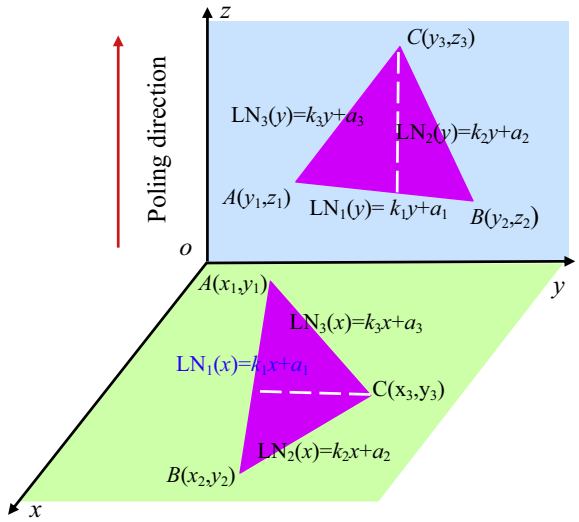

Fig. 1. Triangle ABC in the *oxy* or *oyz* plane and the functions for the three lines AB, BC and AC.

If we further define the following parameters k_i and a_i

$$k_1 = \frac{y_2 - y_1}{x_2 - x_1} \quad k_2 = \frac{y_2 - y_3}{x_2 - x_3}, \quad k_3 = \frac{y_3 - y_1}{x_3 - x_1},$$
$$a_1 = y_1 - x_1 k_1, \quad a_2 = y_2 - x_2 k_2, \quad a_3 = y_3 - x_3 k_3, \tag{4}$$

then the three line functions in Eq. (3) can be expressed as

$$\mathrm{LN}_1(x) = k_1 x + a_1, \quad \mathrm{LN}_2(x) = k_2 x + a_2, \quad \mathrm{LN}_3(x) = k_3 x + a_3. \tag{5}$$

When a uniform load P_I is applied to the arbitrary triangle *ABC* in the *oxy* plane, we can first divide the triangle into two sub-triangles as shown in Fig. 1. Then we apply Eqs. (1) and (2) to these two sub-triangles to obtain

$$u_J(\boldsymbol{x}^f) = P_K \int_{x_1}^{x_3} dx \int_{k_1 x + a_1}^{k_3 x + a_3} u^*_{JK}(\boldsymbol{x}^f; x, y, 0) dy + P_K \int_{x_3}^{x_2} dx \int_{k_1 x + a_1}^{k_2 x + a_2} u^*_{JK}(\boldsymbol{x}^f; x, y, 0) dy, \tag{6a}$$

$$\sigma_{ij}(\boldsymbol{x}^f) = P_K \int_{x_1}^{x_3} dx \int_{k_1 x + a_1}^{k_3 x + a_3} \sigma^*_{ijK}(\boldsymbol{x}^f; x, y, 0) dy + P_K \int_{x_3}^{x_2} dx \int_{k_1 x + a_1}^{k_2 x + a_2} \sigma^*_{ijK}(\boldsymbol{x}^f; x, y, 0) dy. \tag{6b}$$

Two load cases of the triangular element fundamental solutions will be presented in the following subsections.

3.1. Uniform load density P_3 (or P_z) applied over a triangle in oxy plane

When the uniform load P_z over the triangle is along *z*-direction, we denote by u^z_j (u^z_i; $u^z_4 = \phi^z$) and σ^z_{ij} (σ^z_{ij}; $\sigma^z_{i4} = D^z_i$) the induced extended displacements and stresses, with the superscript *z* denoting the direction of the applied load. Based on Eq. (6), the exact solutions of the extended displacements and stresses at any point (*x*, *y*, *z*) can be obtained as

$$u^z_x = P_z \sum_{i=1}^{3} A_i Q^i_{1(z)},$$
$$u^z_y = P_z \sum_{i=1}^{3} A_i Q^i_{2(z)}, \tag{7a}$$
$$u^z_K = -P_z \sum_{i=1}^{3} [\alpha_{i,K-2} A_i Q^i_{3(z)}].$$

In the last equation of Eq. (7a), $K = 3, 4$. When *K* equals 3, the left-hand side of this equation corresponds to u^z_z; when *K* equals 4, it corresponds to ϕ^z. The functions $Q^i_{l(z)}$ in Eq. (7a) and in Eqs. (7b) and (7c) below depend on various parameters as well as variables *x*, *y* and *z*, and their exact closed-form expressions are given in Eq. (A1) of Appendix A. The coefficients A_i and α_{im} ($m = 1, 2$) are material-related coefficients given in Ding et al. [8].

The corresponding extended stresses can be expressed as

$$\begin{aligned}
\sigma_{xx}^{z} &= P_z(c_{11}-c_{12})\sum_{i=1}^{3}A_iQ_{4(z)}^{i} + P_z\sum_{i=1}^{3}A_i\xi_iQ_{5(z)}^{i},\\
\sigma_{yy}^{z} &= P_z(c_{11}-c_{12})\sum_{i=1}^{3}A_iQ_{6(z)}^{i} + P_z\sum_{i=1}^{3}A_i\xi_iQ_{5(z)}^{i},\\
\tau_{xy}^{z} &= -2P_zc_{66}\sum_{i=1}^{3}A_iQ_{7(z)}^{i},
\end{aligned} \tag{7b}$$

$$\begin{aligned}
\sigma_{xK}^{z} &= P_z\sum_{i=1}^{3}\omega_{i,K-2}A_iQ_{8(z)}^{i},\\
\sigma_{yK}^{z} &= P_z\sum_{i=1}^{3}\omega_{i,K-2}A_iQ_{9(z)}^{i},\\
\sigma_{zK}^{z} &= P_z\sum_{i=1}^{3}\vartheta_{i,K-2}A_iQ_{5(z)}^{i}.
\end{aligned} \tag{7c}$$

In Eq. (7b), c_{ij} are the elastic constants. In Eq. (7c), $K = 3, 4$. When K equals 3, the left-hand side of Eq. (7c) corresponds to $\sigma_{xz}^{z}, \sigma_{yz}^{z}, \sigma_{zz}^{z}$; when K equals 4, it corresponds to D_x^z, D_y^z, D_z^z. Also in Eqs. (7b) and (7c), $\xi_i, \omega_{im}, \vartheta_{im}$ ($m = 1, 2$) are all material related constants given in Ding et al. [8].

We further remark that the material-related coefficients A_i ($i = 1$–3) in Eq. (7) can be solved from the following equations [8,18]:

$$\sum_{i=1}^{3}A_i = 0, \quad 4\pi\sum_{i=1}^{3}\vartheta_{i1}A_i = -1, \quad 4\pi\sum_{i=1}^{3}\vartheta_{i2}A_i = 0. \tag{8}$$

It should be pointed out that, when the uniform load density P_4 (the normal electric displacement ω) is applied over the triangle in the *oxy* plane, the induced extended displacements and stresses at any internal point (x, y, z) have the same expressions as Eq. (7), except that we should replace the material-related coefficients A_i by the material-related coefficients B_i, with B_i ($i = 1$–3) being solved from the following equations

$$\sum_{i=1}^{3}B_i = 0, \quad 4\pi\sum_{i=1}^{3}\vartheta_{i1}B_i = 0, \quad 4\pi\sum_{i=1}^{3}\vartheta_{i2}B_i = 1. \tag{9}$$

3.2. Uniform load density P_1 (P_x) along x-direction over a triangle in oxy plane

If the extended load $P_I = P_1$ over the triangle is along x-direction, we denote by u_J^x (u_i^x; $u_4^x = \phi^x$) and σ_{IJ}^x (σ_{ij}^x; $\sigma_{i4}^x = D_i^x$) the extended displacements and the extended stresses, with the superscript x denoting the direction of the applied load. Using Eq. (6), the exact closed-form solutions of the extended displacements and stresses at any internal point (x, y, z) can be obtained as

$$\begin{aligned}
u_x^x &= -P_xD_4Q_{1(x)} + P_x\sum_{i=1}^{3}D_iQ_{2(x)}^{i},\\
u_y^x &= -P_xD_4Q_{3(x)} - P_x\sum_{i=1}^{3}D_iQ_{3(x)}^{i},\\
u_K^x &= P_xx\sum_{i=1}^{3}\left[\alpha_{i,K-2}D_iQ_{4(x)}^{i}\right].
\end{aligned} \tag{10a}$$

In the last equation of Eq. (10a), $K = 3, 4$. When K equals 3, the left-hand side of this equation corresponds to u_z^x; when K equals 4, it corresponds to ϕ^x. The functions $Q_{I(x)}^{i}$ in Eq. (10a) and in Eqs. (10b) and (10c), which depend on variables x, y and z are given in Eq. (A2) of Appendix A,

$$\begin{aligned}
\sigma_{xx}^{x} &= P_x(c_{11}-c_{12})D_4Q_{5(x)} + P_x\sum_{i=1}^{3}D_i\left[\xi_iQ_{6(x)}^{i} - (c_{11}-c_{12})Q_{7(x)}^{i}\right],\\
\sigma_{yy}^{x} &= P_x(c_{11}-c_{12})D_4Q_{5(x)} + P_x\sum_{i=1}^{3}D_i\left[\xi_iQ_{6(x)}^{i} - (c_{11}-c_{12})Q_{5(x)}^{i}\right],\\
\sigma_{xy}^{x} &= P_xc_{66}D_4(Q_{8(x)} - Q_{9(x)}) - 2c_{66}P_x\sum_{i=1}^{3}D_iQ_{9(x)}^{i},
\end{aligned} \tag{10b}$$

$$\sigma_{xK}^{x} = -P_x\omega_{4,K-2}D_4Q_{10(x)} + P_x\sum_{i=1}^{3}\omega_{i,K-2}D_iQ_{11(x)}^{i},$$
$$\sigma_{yK}^{x} = -P_x\omega_{4,K-2}D_4Q_{12(x)} - P_x\sum_{i=1}^{3}\omega_{i,K-2}D_iQ_{12(x)}^{i}, \tag{10c}$$
$$\sigma_{zK}^{x} = P_x\sum_{i=1}^{3}\vartheta_{i,K-2}D_iQ_{6(x)}^{i}.$$

In Eq. (10c), ω_{4m} (m = 1, 2) is a material related constants corresponding to eigenvalue s_4 (Ding et al. [8]), and K = 3, 4. When K equals 3, the left-hand side of Eq. (10c) corresponds to $\sigma_{xz}^{x}, \sigma_{yz}^{x}, \sigma_{zz}^{x}$; when K equals 4, it corresponds to D_x^x, D_y^x, D_z^x. The material-related coefficient D_J (J = 1–4) are given in Ding et al. [8] are determined by (m = 1, 2)

$$\sum_{i=1}^{3}\alpha_{im}D_i = 0, \quad s_4D_4 + \sum_{i=1}^{3}s_iD_i = 0, \quad 2\pi c_{44}s_4D_4 - 2\pi\sum_{i=1}^{3}\omega_{i1}D_i = -1, \tag{10d}$$

where s_J (J = 1–4) are the roots of the material characteristic equation, which depend on the elastic constants c_{ij}, the piezoelectric constants e_{ij} and the dielectric constants ε_{ij} [8,18].

It is pointed out that by simply switching x and y in Eq. (10), one can then obtain the exact closed-form solutions corresponding to the uniform load $P_I = P_2$ which is parallel to the y-axis. In other words, the relationship between these two solutions is

$$\begin{aligned} &u_x^y = u_y^x, \quad u_y^y = u_x^x, \quad u_z^y = u_z^x, \\ &\sigma_{xx}^y = \sigma_{yy}^x, \quad \sigma_{yy}^y = \sigma_{xx}^x, \quad \sigma_{zz}^y = \sigma_{zz}^x, \\ &\tau_{xy}^y = -\tau_{xy}^x, \quad \tau_{xz}^y = \tau_{yz}^x, \quad \tau_{yz}^y = -\tau_{xz}^x. \end{aligned} \tag{11}$$

4. Fundamental solutions for triangle elements in the *oyz* plane

We now consider the case where the triangle element is in the *oyz* plane, i.e., perpendicular to the isotropic plane, as shown in Fig. 1. We denote the three triangle vertices by $A(y_1, z_1)$, $B(y_2, z_2)$ and $C(y_3, z_3)$, and the three straight-lines by $LN_1(y)$, $LN_2(y)$ and $LN_3(y)$ which are expressed as

$$\begin{aligned} LN_1(y) &= z_1 + \frac{z_2 - z_1}{y_2 - y_1}(y - y_1), \\ LN_2(y) &= z_2 + \frac{z_3 - z_2}{y_3 - y_2}(y - y_2), \\ LN_3(y) &= z_3 + \frac{z_3 - z_1}{y_3 - y_1}(y - y_3). \end{aligned} \tag{12}$$

Defining also

$$k_1 = \frac{z_2 - z_1}{y_2 - y_1} \quad k_2 = \frac{z_2 - z_3}{y_2 - y_3}, \quad k_3 = \frac{z_3 - z_1}{y_3 - y_1}, \quad a_1 = z_1 - y_1k_1, \quad a_2 = z_2 - y_2k_2, \quad a_3 = z_3 - y_3k_3, \tag{13}$$

then the functions $LN_i(y)$ can be expressed as

$$LN_1(y) = k_1y + a_1, \quad LN_2(y) = k_2y + a_2, \quad LN_3(y) = k_3y + a_3. \tag{14}$$

The extended displacement and stress fields at any point (x, y, z) under uniformly distributed load P_I over this triangle ABC can be expressed in terms of the following integrals (by dividing this triangle into two sub-triangles):

$$u_J(\boldsymbol{y}^f) = P_I\int_{y_1}^{y_3}dy\int_{k_1y+a_1}^{k_3y+a_3}u_{JI}^*(\boldsymbol{y}^f;0,y,z)dz + P_I\int_{y_3}^{y_2}dy\int_{k_1y+a_1}^{k_2y+a_2}u_{JI}^*(\boldsymbol{y}^f;0,y,z)dz, \tag{15a}$$

$$\sigma_{ij}(\boldsymbol{y}^f) = P_I\int_{y_1}^{y_3}dy\int_{k_1y+a_1}^{k_3y+a_3}\sigma_{ijI}^*(\boldsymbol{y}^f;0,y,z)dz + P_I\int_{y_3}^{y_2}dy\int_{k_1y+a_1}^{k_2y+a_2}\sigma_{ijI}^*(\boldsymbol{y}^f;0,y,z)dz. \tag{15b}$$

Similarly, we derive the exact closed-form solutions for the following two load cases.

4.1. Uniform load density P_I (P_x) along x-direction over a triangle in the oyz plane

For the extended load P_x along x-axis and uniformly distributed over the triangle, we can obtain, from Eq. (15), the extended displacements and the extended stresses at any point (x, y, z) in the infinite body. The results can be also expressed by Eq. (10), but with different $Q_{I(x)}$ and $Q_{I(x)}^{i}$ as given in Eq. (A3) of Appendix A.

We also mention that the solution corresponding to the uniform load $P_I = P_y$ along y-axis in the *oyz* plane can be obtained by a simple switch between x and y as shown in Eq. (11).

4.2. Uniform load density P_z along z-direction over a triangle in the oyz plane

If the uniform load P_z is along z-direction in the oyz plane, then, according to Eq. (15), the extended displacements and stresses at any point (x, y, z) can be also expressed as in Eq. (7). The difference is just that the functions $Q^i_{l(z)}$ are different, which are given in Eq. (A4) of Appendix A.

Similarly, when the uniform load density P_4 is applied over a triangle in the oyz plane, the exact closed-form solutions of the extended displacements and stresses at any point (x, y, z) have the same expressions as Eq. (7), with A_i being replaced by B_i, and the functions $Q^i_{l(z)}$ being given in Eq. (A4) of Appendix A.

5. Numerical results

5.1. Validation of the solution

In this section, we first verify the correctness of the obtained solutions by using the piezoelectric material PZT-6B, with the material constants listed in Table 1.

Fig. 2 show an inner square ABCD (10 m × 10 m) in the transversely isotropic oxy plane, with its four corners at $A(-5, -5, 0)$, $B(5, -5, 0)$, $C(-5, 5, 0)$ and $D(5, 5, 0)$. A uniform force P_z = 1.0 Pa along z-direction is applied over this square. The extended displacements and stresses are calculated by the following three methods of superposition:

Method of superposition 1. Using the Green's function in Zhao et al. [18,26], the extended displacements and stresses at an arbitrary point are calculated by direct integration over the square ABCD;

Method of superposition 2: Using the present solutions in this paper, the extended displacements and stresses at an arbitrary point are obtained by adding those corresponding to the two triangles ABC and CDA (Fig. 2);

Method of superposition 3: Similar to the method of superposition 2, the square is divided into four triangles as labeled by 1, 2, 3, and 4 in Fig. 2. The extended displacements and stresses are obtained by adding these from the four triangles.

Based on the above three methods of superposition, we have calculated the extended displacements and stresses from $(-2, 0, -1)$ to $(2, 0, -1)$. It is found that the three methods of superposition give exactly the same results as those shown in Fig. 3(a) and (b) using method of superposition 2. Therefore, our exact closed-form solution is correct.

5.2. Solutions due to loads over a right triangle

Assume that there is a right triangle AOB in the transverse isotropic oxy plane or a right triangle BOC vertical to that, as shown in Fig. 4. Uniform loads P_z = 1.0 Pa and P_x = 1.0 Pa are respectively applied to these two triangles. Here, we present the variation of the following five quantities as in Wang et al. [27]: the whole elastic displacement u, the electric potential ϕ, the hydrostatic stress σ_h, the effective stress σ_e, the whole electric displacement D

$$u = \sqrt{u_x^2 + u_y^2 + u_z^2},\ \sigma_h = \frac{\sigma_{xx} + \sigma_{yy} + \sigma_{zz}}{3},$$
$$\sigma_e = \left(\frac{1}{2}\left[(\sigma_{xx} - \sigma_{yy})^2 + (\sigma_{xx} - \sigma_{yy})^2 + (\sigma_{xx} - \sigma_{yy})^2\right] + 3\left(\sigma_{xy}^2 + \sigma_{yz}^2 + \sigma_{xz}^2\right)\right)^{1/2},\ D = \sqrt{D_x^2 + D_y^2 + D_z^2}. \tag{16}$$

Case 1 (*Uniform load P_z = 1.0 Pa over the right triangle AOB*). Based on our exact closed-form solutions, the extended displacements and stresses within the square domain of $-5\ \text{m} \leqslant (x, y) \leqslant 5\ \text{m}$ are calculated. The results show that $u_z > u_x > u_y$ with the magnitude of the whole elastic displacement being almost the same as that of u_z. Also the contours of the whole elastic displacement u and electric potential ϕ are very similar to each other, so we just show the contour of the whole elastic displacement, as in Fig. 5a. It can be seen that both of u and ϕ reach their maximum values at the centre of the triangle, with their values being 3.0×10^{-12} m and 3.0×10^{-3} V, respectively. Fig. 5b presents the whole electric displacement D in the oxy plane with its maximum being at the edge of the triangle, whilst Fig. 5c plots the distribution of the effective stress σ_e and the hydrostatic stress σ_h along the line from $(-1, 0.5, -1)$ to $(1, 0.5, -1)$ m.

Case 2 (*Uniform load P_x = 1.0 Pa over the right triangle AOB*). Under uniform load P_x = 1.0 Pa over the right triangle AOB, we find that the magnitude of the elastic displacement components satisfies $u_x > u_y > u_z$. The whole elastic displacement u reaches its maximum value 4.25×10^{-12} m at the centre of the triangle, which is larger than that under the corresponding vertical load, as shown in Fig. 6a. Meanwhile, Fig. 6b shows that, when compared to the vertical load case (the same shape as

Table 1
Material coefficients of piezoelectric PZT-6B.

c_{11} (10^9 N/m^2)	c_{12} (10^9 N/m^2)	c_{13} (10^9 N/m^2)	c_{33} (10^9 N/m^2)	C_{44} (10^9 N/m^2)
168	60	60	163	27.1
e_{13} (C/m^2)	e_{33} (C/m^2)	e_{15} (C/m^2)	ε_{11} (10^{-9}C/(V m))	ε_{33} (10^{-9}C/(V m))
−0.9	7.1	4.6	3.6	3.4

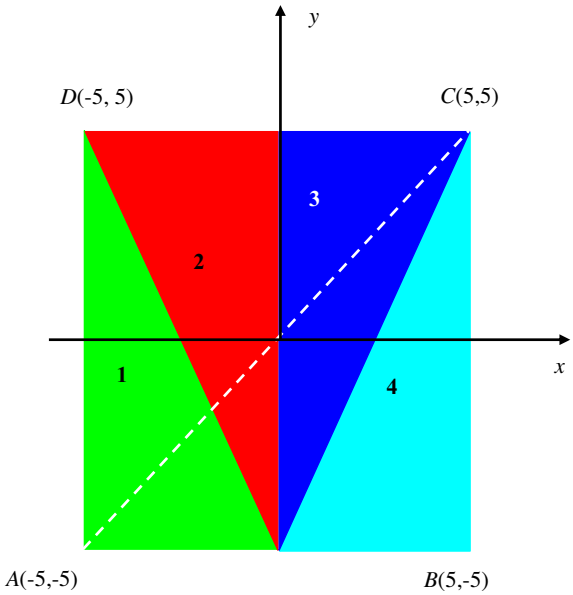

Fig. 2. A uniform load $P_z = 1.0$ Pa over the rectangle ABCD (10 m × 10 m) on the *oxy* plane. This problem is solved by three different methods of superposition discussed in detail in the text to validate the exact closed-form solutions presented in this paper.

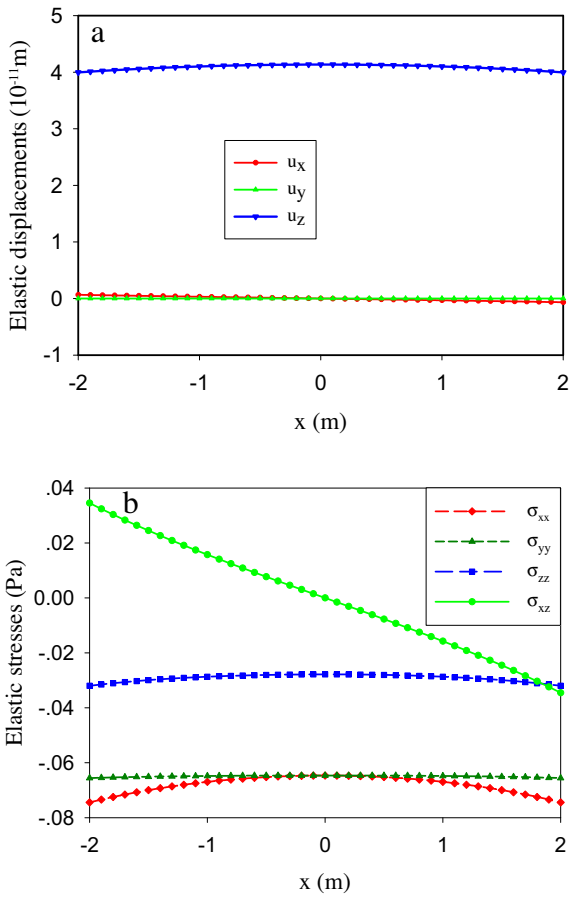

Fig. 3. (a) The elastic displacements u_x, u_y, and u_z along the line from (−2, 0, −1) to (2, 0, −1) m due to the uniform load $P_z = 1.0$ Pa over the rectangle ABCD as shown in Fig. 2, using Method of superposition 2. (b) The elastic stresses along the line from (−2, 0, −1) to (2, 0, −1) m due to the uniform load $P_z = 1.0$ Pa over the rectangle ABCD as shown in Fig. 2, using Method of superposition 2.

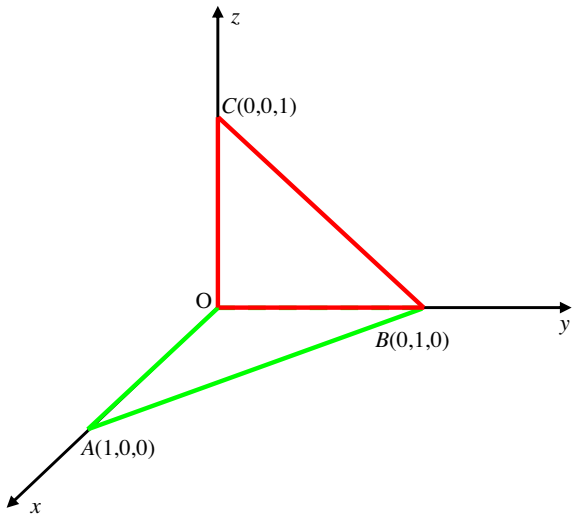

Fig. 4. A horizontal right triangle AOB and a vertical right triangle BOC over which uniform load $P_z = 1.0$ Pa or $P_x = 1.0$ Pa is applied.

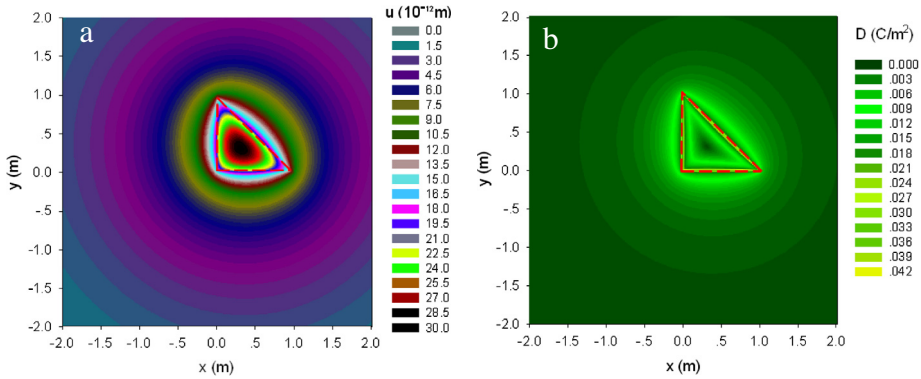

Fig. 5a,b. Contours of the elastic displacement u (10^{-12} m) in (a), and the electric displacement D (C/m^2) in (b) in the *oxy* plane, induced by a uniform vertical load $P_z = 1.0$ Pa within the right triangle AOB, as shown in Fig. 4 (also shown here by the dashed straight lines).

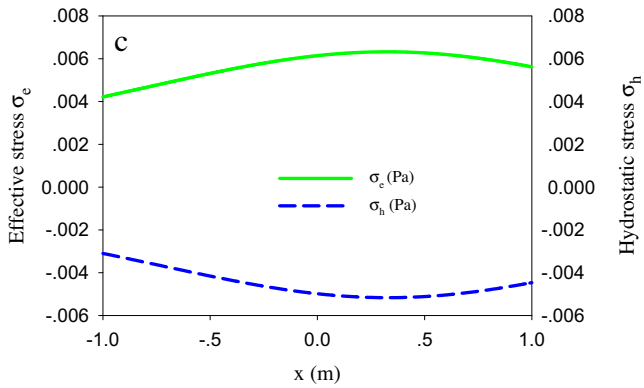

Fig. 5c. The effective stress σ_e (Pa) and hydrostatic stress σ_h (Pa) along the line from (−1, 0.5, −1) to (1, 0.5, −1) m due to the uniform load $P_z = 1.0$ Pa over the right triangle AOB shown in Fig. 4.

u in Fig. 6a), not only the contour shape but also the sign of the electric potential are completely different. It can be seen that at some points the electric potential are negative. While not showing here, we noticed that the shape of the hydrostatic stress σ_h is very similar to the electric potential ϕ with a maximum value of σ_h being 0.53 Pa at the edge of the triangle. Fig. 6c displays the contours of the effective stress σ_e, which reach a maximum value of 0.965 Pa at the edge of the right triangle. Fig. 6d shows the electric displacement D and the hydrostatic stress σ_h along the line from $(-1, 0.5, -1)$ to $(1, 0.5, -1)$ m.

Case 3 (*Uniform load P_z = 1.0 Pa over the right triangle BOC*). Fig. 7(a)–(d) show the whole displacement u, hydrostatic stress σ_h, effective stress σ_e and the electric displacement D in the *oyz* plane within the domain of $-2\,\text{m} \leqslant (x, y) \leqslant 2\,\text{m}$. It is observed that at the centre of the right triangle BOC, the elastic displacement u reaches its maximum value of 4.05×10^{-12} m, and the contour of the electric potential ϕ is also similar to the whole elastic displacement u, with a

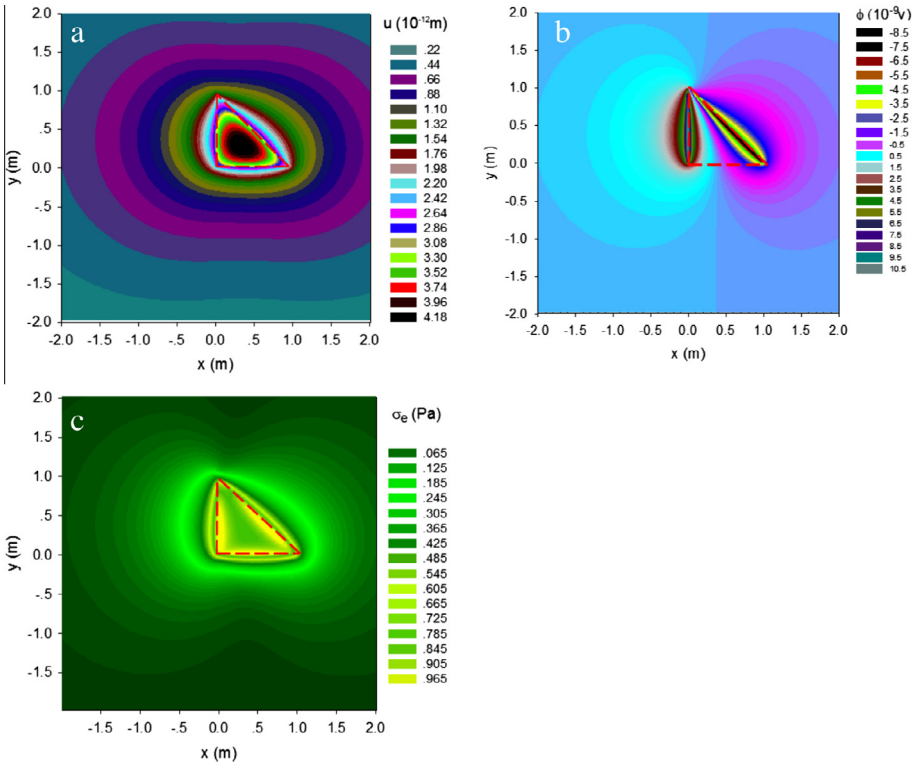

Fig. 6a,b,c. Contours of the elastic displacement u (10^{-12} m) in (a), electric potential ϕ (10^{-9} V) in (b), the effective stress σ_e (Pa) in (c) in the *oxy* plane, induced by the uniform shear load P_x = 1.0 Pa within the right triangle AOB, as shown in Fig. 4 (also shown here by the dashed straight lines).

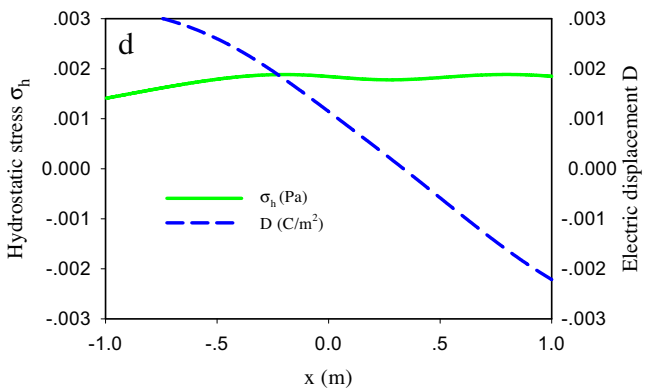

Fig. 6d. The electric displacement D (C/m^2) and hydrostatic stress σ_h (Pa) along the line from $(-1, 0.5, -1)$ to $(1, 0.5, -1)$ m due to the uniform load P_x = 1.0 Pa over the right triangle AOB as shown in Fig. 4.

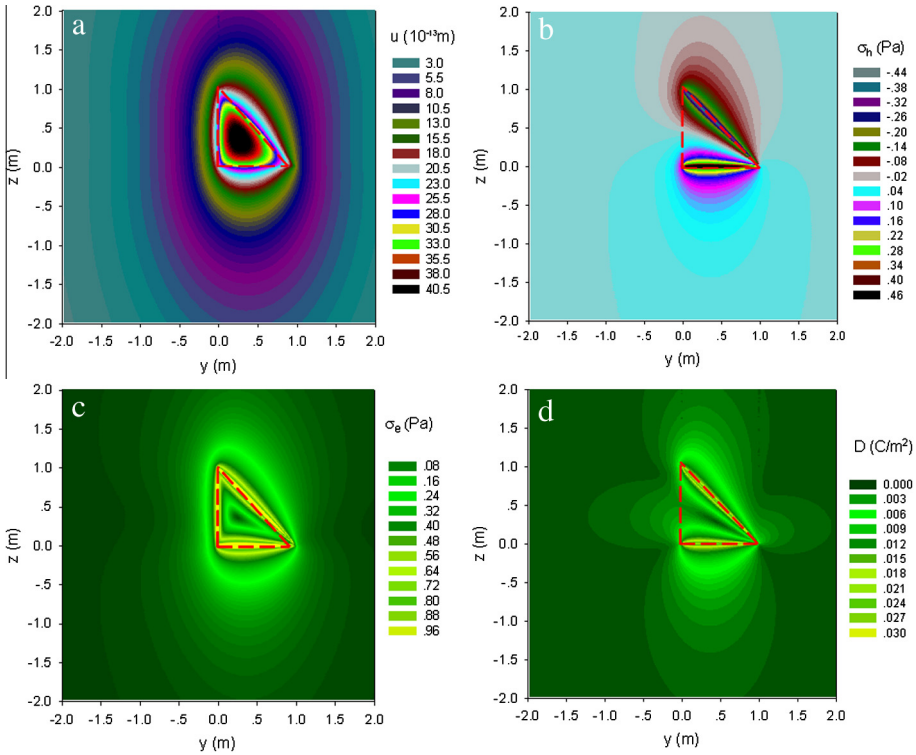

Fig. 7. Contours of the elastic displacement u (10^{-13} m) in (a), hydrostatic stress σ_h (Pa) in (b), effective stress σ_e (Pa) in (c), and the electric displacement D (C/m^2) in (d) in the *oyz* plane, induced by a uniform vertical load P_z = 1.0 Pa within the right triangle BOC as shown in Fig. 4 (also shown here by the dashed straight lines).

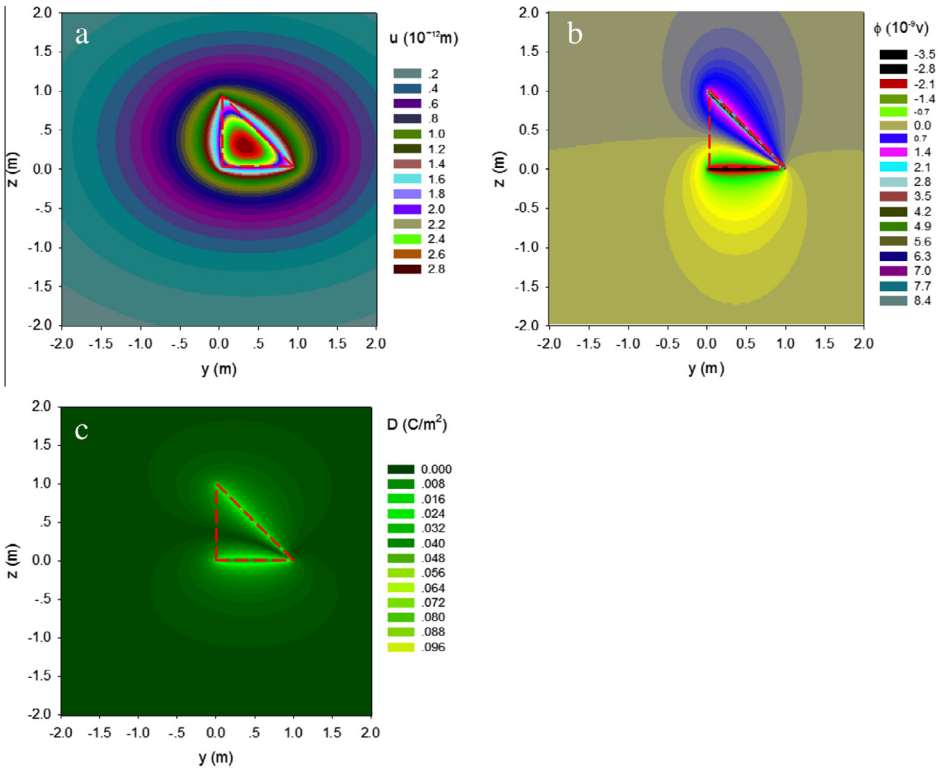

Fig. 8a,b,c. Contours of the elastic displacement u (10^{-12} m) in (a), the electric potential ϕ (10^{-9} V) in (b), and the electric displacement D (C/m^2) in (c) in the *oyz* plane, induced by a uniform shear load P_x = 1.0 Pa within the right triangle BOC, as shown in Fig. 4 (also shown here by the dashed straight lines).

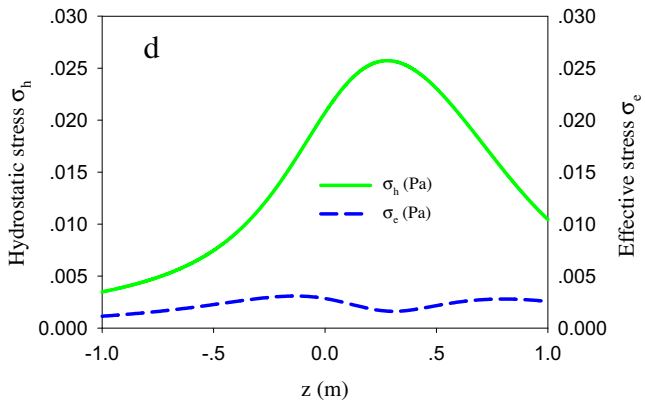

Fig. 8d. The effective stress σ_e (Pa) and hydrostatic stress σ_h (Pa) along the line from (−1, 0.5, −1) to (−1, 0.5, 1) m due to the uniform load P_x = 1.0 Pa over the right triangle BOC as shown in Fig. 4.

maximum value of 5.4×10^{-7} V at the centre of BOC. Also, σ_h, σ_e and D all reach their maximum (absolute) values at the edge of the right triangle BOC, which are, respectively, 0.46 Pa, 0.96 Pa and 0.03 C/m^2. Compared to the same load over the right triangle AOB, we have here the elastic displacement magnitude relation $u_x > u_y > u_z$.

Case 4 (*Uniform load P_x = 1.0 Pa over the right triangle BOC*). Fig. 8a shows, under this load, that the whole elastic displacement reaches its maximum value of 2.8×10^{-12} m at the centre of the triangle, which is smaller than that under a vertical load. In this case, we have the magnitude relation as $u_z > u_x > u_y$. The contours of the electric potential ϕ are plotted in Fig. 8b, whilst Fig. 8c presents those of the electric displacement D with a maximum value of 0.096 C/m^2 at the edge of the triangle BOC. Fig. 8d shows the distribution of the hydrostatic stress σ_h and the effective stress σ_e from (−1, 0.5, −1) to (−1, 0.5, 1) m. It can be seen that the hydrostatic stress is far larger than the effective stress in this domain.

6. Concluding remarks

In this paper, the fundamental solutions for uniformly distributed extended loads over a triangle in transversely isotropic piezoelectric materials are obtained. Three methods of superposition are used to validate the derived exact closed-form solution. Numerical results show that the maximum values of the extended stresses all occur at the edge of the triangle.

The method proposed in the present paper is versatile and can be utilized to derive the fundamental solutions for other kinds of elements, such as circle, rectangle, etc. applied by arbitrarily distributed loads.

When a transversely isotropic infinite body is subjected to an arbitrarily shaped load over a finite region, solutions to this general case can be obtained by the method of superposition where one divides the load area into many triangles or other kinds of elements. Therefore, the exact closed-form solution presented in the paper should be very useful in analyzing the behavior of transversely isotropic materials under general distributed loads over an arbitrarily shaped area.

Acknowledgements

The work was supported by the National Natural Science Foundation of China (Nos. 11102186, 11072221, 11172273), and the Bairen Program in Henan Province. The authors would also like to thank the reviewers and the Editor of the journal for their useful comments and suggestion on the original version of this article.

Appendix A. Functions and parameters involved in Eqs. (7) and (10)

A.1. A triangle on the oxy plane

We consider an infinite piezoelectric body under a uniformly distributed load over a triangle *ABC*, which is located on plane of transverse isotropy. We denote the vertex coordinates of the triangle as $A(x_1, y_1)$, $A(x_2, y_2)$ and $C(x_3, y_3)$. The displacements and the stresses at any point (x, y, z) induced by this uniform load over the triangle can be expressed by Eq. (7), with the related functions being defined as below:

(a) The uniform load is along z-direction in the oxy plane
For this case, the functions $Q^i_{k(z)}$ in Eq. (7) can be expressed as:

$$
\begin{aligned}
Q^j_{1(z)} &= \frac{1}{2}\sum_{m=1}^{6}\begin{bmatrix} 2(-1)^{m+1}(G_{1m} + l_{[2m]}G_{2m} + G^j_{3m}) + (-1)^m H_{2m} \\ +2s_j z k_{[2m]}(-1)^m H^j_{3m} + (L^j_{1m} + L^j_{2m}) \end{bmatrix}, \\
Q^j_{2(z)} &= \frac{1}{2}\sum_{m=1}^{6}\left[2(-1)^m G_{4m} + (-1)^m(l_{[2m]}H_{1m} - 2s_j z H^j_{3m} + H^j_{3m}) + L^j_{2m}\right], \\
Q^j_{3(z)} &= \frac{1}{2}\sum_{m=1}^{6}\left[2(-1)^m(H^j_{5m} - H^j_{6m}) + L^j_{3m}\right], \\
Q^j_{4(z)} &= \frac{1}{2}\sum_{m=1}^{6}\left[2(-1)^m G_{2m} + k_{[2m]}(-1)^m H_{1m} + L^j_{4m} + L^j_{5m}\right], \\
Q^j_{5(z)} &= \frac{1}{2}\sum_{m=1}^{6} L^j_{4m}, \quad Q^j_{6(z)} = \frac{1}{2}\sum_{m=1}^{6}\left[2(-1)^{m+1}G_{2m} + (-1)^{m+1}k_{[2m]}H_{1m} + L^j_{5m}\right], \\
Q^j_{7(z)} &= \frac{1}{2}\sum_{m=1}^{6}\left[2(-1)^m G_{2m} + (-1)^{m+1}H_{1m} + iL^j_{5m}\right], \\
Q^j_{8(z)} &= \frac{1}{2}\sum_{m=1}^{6}\left[2(-1)^m k_{[2m]}H^j_{3m} + L^j_{6m}\right], \quad Q^j_{9(z)} = \sum_{m=1}^{6}(-1)^{m+1}H^j_{3m}.
\end{aligned}
\tag{A1}
$$

(b) The uniform load is along x-direction in the oxy plane

For this case, the induced extended displacements and stresses are given by Eq. (10) with the functions being

$$
\begin{aligned}
Q_{1(x)} &= \tfrac{1}{2}\sum_{m=1}^{6}\begin{bmatrix} 2s_j z(-1)^{m+1}G_{2m} + (-1)^{m+1}k_{[2m]}s_j z H_{1m} \\ +(-1)^{m+1}H^j_{8m} + 2(-1)^{m+1}M^j_{2m} + s_j z L^j_{5m} \end{bmatrix}, \quad j = 4, \\
Q_{3(x)} &= (-1)^{m+1}s_4 z G_{4m} + (-1)^m(s_4 z H_{1m} - k_{[2m]}H^j_{8m}) + (-1)^m M^j_{1m} + \tfrac{s_4 z L^j_{6m}}{2}, \quad j = 4, \\
Q_{5(x)} &= \sum_{m=1}^{6}\left[(-1)^m H^j_{7m} + (-1)^{m+1}(s_j z M_{3m} + M^j_{4m})\right], \quad j = 4, \\
Q_{8(x)} &= \sum_{m=1}^{6}(-1)^{m+1}H^j_{3m}, \quad j = 4, \\
Q_{9(x)} &= \sum_{m=1}^{6}\left[(-1)^{m+1}k_{[2m]}H^j_{7m} + (-1)^m(M_{7m} + M^j_{8m})\right], \quad j = 4, \\
Q_{10(x)} &\ \tfrac{1}{2}\sum_{m=1}^{6}\left[2(-1)^{m+1}G_{2m} + (-1)^{m+1}k_{[2m]}H_{1m} + L^j_{5m}\right], \quad j = 4, \\
Q_{12(x)} &= \tfrac{1}{2}\sum_{m=1}^{6}\begin{bmatrix} (-1)^{m+1}(2G^j_{6m} + 4G^j_{7m}) + (-1)^m(H^j_{10m} - H^j_{11m} - H^j_{12m} + H^j_{13m}) \\ +2(-1)^m M^j_{1m} + (L^j_{7m} + L^j_{8m}) \end{bmatrix}, \quad j = 4, \\
Q^j_{2(x)} &= \tfrac{1}{2}\sum_{m=1}^{6}\begin{bmatrix} 2s_j z(-1)^m(G_{1m} - G_{2m}) + 2(-1)^m M^j_{2m} \\ +(-1)^m(k_{[2m]}s_j z H_{1m} - 2H^j_{3m} + 2H^j_{5m} + 2H^j_{8m}) \\ +s_j z(L^j_{3m} + L^j_{6m}) \end{bmatrix}, \\
Q^j_{3(x)} &= \tfrac{1}{2}\sum_{m=1}^{6}\begin{bmatrix} 2(-1)^{m+1}s_j z G_{4m} + 2(-1)^m(s_j z H_{1m} - k_{[2m]}H^j_{8m}) \\ +2(-1)^m M^j_{1m} + s_j z L^j_{6m} \end{bmatrix}, \\
Q^j_{4(x)} &= \tfrac{1}{2}\sum_{m=1}^{6}\begin{bmatrix} 2(-1)^{m+1}(G_{1m} + l_{[2m]}G_{2m} + G^j_{3m}) \\ +(-1)^m(H_{2m} + 2k_{[2m]}s_j z H^j_{3m}) + (L^j_{1m} + L^j_{2m}) \end{bmatrix}, \\
Q^j_{5(x)} &= \sum_{m=1}^{6}\left[(-1)^m H^j_{7m} + (-1)^{m+1}(s_j z M_{3m} + M^j_{4m})\right], \\
Q^j_{6(x)} &= \tfrac{1}{2}\sum_{m=1}^{6}\left[2(-1)^m k_{[2m]}H^j_{3m} + L^j_{6m}\right], \\
Q^j_{7(x)} &= \sum_{m=1}^{6}\left[(-1)^m H^j_{9m} + (-1)^{m+1}(M^j_{5m} + M^j_{6m})\right], \quad Q^j_{8(x)} = Q^j_{9(z)}, \\
Q^j_{9(x)} &= \sum_{m=1}^{6}\left[(-1)^{m+1}k_{[2m]}H^j_{7m} + (-1)^m(M_{7m} + M^j_{8m})\right], \\
Q^j_{11(x)} &= Q^j_{4(z)}, \\
Q^j_{12(x)} &= \tfrac{1}{2}\sum_{m=1}^{6}\begin{bmatrix} (-1)^{m+1}(2G^j_{6m} + 4G^j_{7m}) + (-1)^m(H^j_{10m} - H^j_{11m} - H^j_{12m} + H^j_{13m}) \\ +2(-1)^m M^j_{1m} + (L^j_{7m} + L^j_{8m}) \end{bmatrix}.
\end{aligned}
\tag{A2}
$$

A.2. A triangle on the oyz plane

We now assume that the infinite elastic body is under a uniform load over a triangle which is perpendicular to the plane of transverse isotropy (actually located in the *oyz* plane). The triangle is named as *ABC* with its vertex coordinates being at $A(y_1, z_1)$, $B(y_2, z_2)$ and $C(y_3, z_3)$. The induced displacements and the stresses at any point (x, y, z) can be expressed by Eq. (8), with the involved functions being listed below.

(a) The uniform load is along *x*-direction in the *oyz* plane
For this case the functions $Q^j_{k(x)}$ $(Q_{k(x)})$ in Eq. (10) can be found as:

$$
\begin{aligned}
Q_{1(x)} &= \tfrac{s_j}{2}\left[(k_1^2-k_3^2)y_1+(k_2^2-k_1^2)y_2+(k_3^2-k_2^2)y_3\right]+\tfrac{s_j}{2}\sum_{n=1}^{3}[2xG_{9n}+H_{14n}] \\
&\quad +\tfrac{1}{4}\sum_{m=1}^{6}\left[2(-1)^m(2H^j_{16m}+H^j_{17m})+2(-1)^{m+1}(s_jM_{10m}-M^j_{11m})+L^j_{9m}\right], \quad j=4, \\
Q_{3(x)} &= \frac{s_j}{2}\sum_{n=1}^{3}(2G_{10n}+H_{19n}+xM_{12n})+\frac{x}{4}\sum_{m=1}^{6}\begin{bmatrix}4(-1)^m k_{[2m]}H^j_{18m} \\ +2(-1)^{m+1}g_mM^j_{9m}+L^j_{11m}\end{bmatrix}, \quad j=4, \\
Q_{5(x)} &= s_j\sum_{n=1}^{3}G_{9n}+\frac{1}{2}\sum_{m=1}^{6}\left[2s_jxM_{13m}+2(-1)^{m+1}xM^j_{14m}+L^j_{13m}\right], \quad j=4, \\
Q_{8(x)} &= \frac{1}{2}\sum_{m=1}^{6}\left[2(-1)^m k_{[2m]}H^j_{15m}+L^j_{16m}\right], \quad j=4, \\
Q_{9(x)} &= \frac{s_j}{2}\sum_{n=1}^{3}H_{19n}+\frac{1}{4}\sum_{m=1}^{6}\left[4(-1)^m k_{[2m]}H^j_{18m}+2(-1)^mM^j_{15m}+2M^j_{16m}+L^j_{17m}\right], \quad j=4, \\
Q_{10(x)} &= \frac{1}{2}\sum_{n=1}^{3}(H_{20n}+2M_{17n})+\frac{1}{2}\sum_{m=1}^{6}\left[2(-1)^{m+1}k^2_{[2m]}s_jH^j_{15m}+2(-1)^{m+1}\frac{\beta_{[2m]}}{s_j}M^j_{9m}+L^j_{18m}\right], \quad j=4, \\
Q_{12(x)} &= \sum_{n=1}^{3}(G_{8n}+2xM_{18n})+\frac{1}{2}\sum_{m=1}^{6}\left[2(-1)^m\frac{x}{s_j}M^j_{9m}+iL^j_{18}\right], \quad j=4, \\
Q^j_{2(x)} &= \tfrac{s_j}{2}\left[(k_3^2-k_1^2)y_1+(k_1^2-k_2^2)y_2+(k_2^2-k_3^2)y_3\right]+\tfrac{s_j}{2}\sum_{n=1}^{3}[2xG_{9n}+H_{14n}] \\
&\quad +\tfrac{1}{4}\sum_{m=1}^{6}[2(-1)^m(H^j_{17m}-2H^j_{18m})+2(-1)^m(s_jM_{10m}-M^j_{11m})+L^j_{10m}], \\
Q^j_{3(x)} &= \frac{s_j}{2}\sum_{n=1}^{3}(2G_{10n}+H_{19n}+xM_{12n})+\frac{x}{4}\sum_{m=1}^{6}\begin{bmatrix}4(-1)^m k_{[2m]}H^j_{18m} \\ +2(-1)^{m+1}g_mM^j_{9m}+L^j_{11m}\end{bmatrix}, \\
Q^j_{4(x)} &= \frac{1}{2}\sum_{n=1}^{3}(2G_{11n}+xH_{20n})+\frac{x}{2}\sum_{m=1}^{6}\left[2(-1)^mH^j_{18m}+L^j_{12m}\right], \\
Q^j_{5(x)} &= s_j\sum_{n=1}^{3}G_{9n}+\frac{1}{2}\sum_{m=1}^{6}\left[2s_jxM_{13m}+2(-1)^{m+1}xM^j_{14m}+L^j_{13m}\right], \\
Q^j_{6(x)} &= \frac{1}{2}\sum_{m=1}^{6}L^j_{14m}, \quad Q^j_{7(x)} = s_j\sum_{n=1}^{3}G_{9n}+\frac{1}{2}\sum_{m=1}^{6}\left[-2s_jxM_{13m}+2(-1)^mxM^j_{14m}+L^j_{15m}\right], \\
Q^j_{9(x)} &= \frac{s_j}{2}\sum_{n=1}^{3}H_{19n}+\frac{1}{4}\sum_{m=1}^{6}\left[4(-1)^m k_{[2m]}H^j_{18m}+2(-1)^mM^j_{15m}+2M^j_{16m}+L^j_{17m}\right], \\
Q^j_{11(x)} &= \frac{1}{2}\sum_{n=1}^{3}[H_{20n}-2M_{17n}]+\frac{1}{2}\sum_{m=1}^{6}\left[\frac{2}{s_j}(-1)^mH^j_{18m}+2(-1)^m\frac{\beta_t}{s_j}M^j_{9m}+L^j_{18m}\right], \\
Q^j_{12(x)} &= \sum_{n=1}^{3}(G_{8n}+2xM_{18n})+\frac{1}{2}\sum_{m=1}^{6}\left[2(-1)^m\frac{x}{s_j}M^j_{9m}+iL^j_{18}\right].
\end{aligned}
\tag{A3}
$$

(b) The uniform load is along *z*-direction in the *oyz* plane

For this case, the involved functions $Q^j_{k(z)}$ in Eq. (7) can be expressed as:

$$
\begin{aligned}
&Q^j_{1(z)} = Q^j_{4(x)},\\
&Q^j_{2(z)} = (k_3-k_1)y_1 + (k_1-k_2)y_2 + (k_2-k_3)y_3 + \tfrac{1}{2}\sum_{m=1}^{3}(2xG_{8m} + H_{21m})\\
&\qquad + \tfrac{1}{2}\sum_{m=1}^{6}\left[\tfrac{2}{s_j}(-1)^m H^j_{16m} + 2(-1)^{m+1}M^j_{9m} + L^j_{19m}\right],\\
&Q^j_{3(z)} = \frac{1}{2}\sum_{m=1}^{6}\left[2(-1)^{m+1}q_{[2m]}H^j_{15m} + \frac{2}{s_j}(-1)^m H^j_{17m} + L^j_{20m}\right],\\
&Q^j_{4(z)} = Q^j_{11(x)}, \quad Q^j_5 = \frac{1}{s_j}\sum_{m=1}^{6}H^j_{15m}, \quad Q^j_{6(z)} = Q^j_{10(x)},\\
&Q^j_{7(z)} = Q^j_{12(x)}, \quad Q^j_{8(z)} = Q^j_{6(x)}, \quad Q^j_{9(z)} = Q^j_{8(x)}.
\end{aligned}
\tag{A4}
$$

In Eqs. (A1)–(A4), G, M, H and L are functions of the coordinates x, y and z, as well as other parameters. Before we present the expressions for functions G, M, H and L, we first define the following symbols, parameters, and some simple functions:

$$
\text{Subscript “}[2m]\text{”} : [2m] = \begin{cases} 1 \text{ if } m = 1 \text{ or } 2; \text{ or } m = 7 \text{ or } 8;\\ 2 \text{ if } \ m = 3 \text{ or } 4;\\ 3 \text{ if } m, = 5 \text{ or } 6. \end{cases}
\tag{A5}
$$

$$
\text{Subscript “}(m)\text{”} : (m) = \begin{cases} 1 \text{ if } \ m = 1 \text{ or } 5;\\ 2 \text{ if } m = 2 \text{ or } 3;\\ 3 \text{ if } m = 4 \text{ or } 6. \end{cases}
\tag{A6}
$$

$$
u_j = \begin{cases} g_1^2 - g_5^2 & (j = 1 \text{ or } 4)\\ g_3^2 - g_2^2 & (j = 2 \text{ or } 5)\\ g_6^2 - g_4^2 & (j = 3 \text{ or } 6) \end{cases},
\tag{A7}
$$

$$
\begin{aligned}
&\mu_m = a_{[2m]} - y + k_{[2m]}x_{(m)},\\
&\alpha_m = a_{[2m]} - y_{(m)} + k_{[2m]}x,\\
&g_m = a_{[2m]} + k_{[2m]}y_{(m)} - z,\\
&\theta^j_m = a_{[2m]} - y + k_{[2m]}[x + (-1)^m i s_j z],\\
&\rho_m = a_{[2m]} - z + k_{[2m]}[y + i(-1)^m x],\\
&\lambda^j_m = x - x_{[2m]} + (-1)^m i s_j z,
\end{aligned}
\tag{A8}
$$

$$
\begin{aligned}
&\vartheta_j = x - x_j,\\
&\beta_j = y - y_j,\\
&\gamma_j = a_j - z,
\end{aligned}
\tag{A9}
$$

$$
\begin{aligned}
&\nu_j = a_j - y + k_j x,\\
&l_j = a_j k_j - k_j y - x,\\
&q_j = a_j + k_j y - z,
\end{aligned}
\tag{A10}
$$

$$
\begin{aligned}
&r^j_i = (x - x_i)^2 + (s_j z)^2, \quad i = 1, 2, 3\\
&h_j = x^2 + (y - y_j)^2,
\end{aligned}
\tag{A11}
$$

$$
\begin{aligned}
&p^j_{m1} = (\mu_{2[2m]-1} + (-1)^m i\vartheta_{[2m]})\begin{bmatrix} (\mu_{2[2m]} + (-1)^m i\vartheta_{[2m]})\nu_{[2m]} + (-1)^m i s_j^2 z^2 \gamma_{[2m]}\\ +(-1)^m i s_j z \gamma_{[2m]}\sqrt{\mu^2_{2[2m]-1} + r^j_{[2m]}} \end{bmatrix},\\
&p^j_{m2} = (\mu_{2[2m]} + (-1)^m i\vartheta_{[2m]})\begin{bmatrix} (\mu_{2[2m]-1} + (-1)^m i\vartheta_{[2m]})\nu_{[2m]} + (-1)^m i s_j^2 z_i^2 z^2 \gamma_{[2m]}\\ +(-1)^m i s_j z \gamma_{[2m]}\sqrt{\mu^2_{2[2m]} + r^j_{[2(m+2)]}} \end{bmatrix},\\
&p^j_m = \log(p^j_{m1}/p^j_{m2}),\\
&f^j_m = \log\left[\frac{\left(x + (-1)^{m+1} i\beta_{2[2m]}\right)\left(s_j^2 g_{2[2m]-1}\rho_m + ix(-1)^{m+1}\beta_{2[2m]-1} + \rho_m s_j\sqrt{(s_j g_{2[2m]-1})^2 + h^j_{[2m]}}\right)}{\left(x + (-1)^{m+1} i\beta_{2[2m]-1}\right)\left(s_j^2 g_{2[2m]}\rho_m + ix(-1)^{m+1}\beta_{2[2m]} + \rho_m s_j\sqrt{(s_j g_{2[2m]})^2 + h^j_{[2(m+2)]}}\right)}\right],
\end{aligned}
\tag{A12}
$$

$$G_{1m} = x_{[2m]} \arctan(\mu_m/\vartheta_{[2m]}), \quad G_{2m} = \frac{\arctan((k_{[2m]}\mu_m - \vartheta_{(m)})/v_{[2m]})}{1 + k_{[2m]}^2}, \tag{A13}$$

$$G_{3m}^j = x_{[2m]} \arctan\left(\frac{s_j \mu_m z}{\vartheta_{(m)}\sqrt{\mu_m + r_{(m)}^j}}\right), \quad G_{4m} = v_{[2m]} G_{2m}, \tag{A14}$$

$$G_{5m} = k_{[2m]} G_{2m}, \quad G_{6m}^j = \frac{k_{[2m]}\left[2v_{[2m]} + \left(1 + k_{[2m]}^2\right)s_j^2 z^2\right]}{\left(1 + k_{[2m]}^2\right)s_j^2 z^2} G_{2m}, \tag{A15}$$

$$G_{7m}^j = \frac{k_{[2m]} v_{[2m]} \sqrt{v_{[2m]}^2 + \left(1 + k_{[2m]}^2\right)s_j^2 z^2} \arctan\left(\frac{k_{[2m]}\mu_m - \vartheta_{(m)}}{\sqrt{v_{[2m]}^2 + \left(1 + k_{[2m]}^2\right)s_j^2 z^2}}\right)}{\left(1 + k_{[2m]}^2\right)^2 s_j^2 z^2}, \tag{A16}$$

$$G_{8j} = \arctan((y - y_j)/x), \quad G_{9j} = [k_j\gamma_j - k_{j-1}\gamma_{j-1} + (k_j^2 - k_{j-1}^2)y]G_{8j}, \tag{A17}$$

$$G_{10j} = [a_j - a_{j-1} + (k_j - k_{j-1})y]G_{8j}, \tag{A18}$$

$$H_{1m} = \frac{\log[\mu_m^2 + \vartheta_{(m)}^2]}{(1 + k_{[2m]}^2)}, \quad H_{2m} = v_{[2m]} H_{1m}, \tag{A19}$$

$$H_{3m}^j = \frac{\log\left[2\left(\frac{k_{[2m]}\mu_m - \vartheta_{(m)}}{\sqrt{1 + k_{[2m]}^2}} + \sqrt{\mu_m^2 + r_{(m)}^j}\right)\right]}{\sqrt{1 + k_{[2m]}^2}}, \quad H_{4m}^j = x_{[2m]} \log\left[-s_j z + \sqrt{\mu_m^2 + r_{(m)}^j}\right], \tag{A20}$$

$$H_{5m}^j = x_{[2m]} \log[-\mu_m + \sqrt{\mu_m^2 + r_{(m)}^j}], \quad H_{6m}^j = v_{[2m]} H_{3m}^j, \quad H_{7m}^j = \frac{k_{[2m]}}{1 + k_{[2m]}^2} H_{3m}^j, \tag{A21}$$

$$H_{6m}^j = v_{[2m]} H_{3m}^j, \quad H_{7m}^j = \frac{k_{[2m]}}{1 + k_{[2m]}^2} H_{3m}^j, \quad H_{8m}^j = \frac{v_{[2m]}}{1 + k_{[2m]}^2} H_{3m}^j, \tag{A22}$$

$$H_{9m}^j = \frac{k_{[2m]}^3}{\sqrt{\left(1 + k_{[2m]}^2\right)^3}} \log\left[2\left(-\frac{\alpha_m + k_{[2m]}^2\beta_{(m)}}{\sqrt{1 + k_{[2m]}^2}} + \sqrt{\alpha_m^2 - k_{[2m]}^2(\beta_{(m)}^2 + s_j^2 z^2)}\right)\right], \tag{A23}$$

$$H_{10m}^j = \frac{(k_{[2m]}^2 - 1)v_{[2m]}^2 - (k_{[2m]}^2 + 1)(x^2 + s_j^2 z^2)}{(k_{[2m]}^2 + 1)s_j^2 z^2} H_{1m}, \tag{A24}$$

$$H_{11m}^j = \frac{(x_{[2m]} - 2x)x_{(m)}}{s_j^2 z^2} \log[\mu_m^2 + \vartheta_{(m)}^2], \tag{A25}$$

$$H_{12m}^j = \frac{(k_{[2m]}^2 - 1)v_{[2m]}^2 - (k_{[2m]}^2 + 1)(x^2 + s_j^2 z^2)}{\left(k_{[2m]}^2 + 1\right)^2 s_j^2 z^2} \log[\mu_m^2 + r_{(m)}^j], \tag{A26}$$

$$H_{13m}^j = \frac{(x_{(m)} - 2x)x_{(m)}}{s_j^2 z^2} \log[\mu_m^2 + r_{(m)}^j], \tag{A27}$$

$$H_{14j} = [k_j\gamma_j - k_{j-1}\gamma_{j-1} + (k_j^2 - k_{j-1}^2)y]\log[h_j], (\text{Note : in both } \gamma \text{ and} k_j, \text{we assign } j = 3 \text{ if } j = 0), \tag{A28}$$

$$H^j_{15m} = \frac{1}{\sqrt{1+(k_{[2m]}s_j)^2}} \log\left[2\left(\frac{s_j^2 k_{[2m]} g_m - \beta_{(m)}}{\sqrt{1+(k_{[2m]}s_j)^2}} + \sqrt{(s_j g_m)^2 + h_{(m)}}\right)\right], \tag{A29}$$

$$H^j_{16m} = s_j^2 k^2_{[2m]} q_{[2m]} H^j_{15m}, \quad H^j_{17m} = \frac{y_{(m)} \log[-q_{[2m]} + \sqrt{q^2_{[2m]} + h_{(m)}}]}{s_j}, \tag{A30}$$

$$H^j_{17m} = \frac{y_{(m)} \log[-q_{[2m]} + \sqrt{q^2_{[2m]} + h_{(m)}}]}{s_j}, \tag{A31}$$

$$H^j_{18m} = \sqrt{1+(s_j k_{[2m]})^2} \log\left[2\left(\frac{s_j^2 k_{[2m]} g_m - \beta_{(m)}}{\sqrt{1+(s_j k_{[2m]})^2}} + \sqrt{(s_j g_m)^2 + h_{(m)}}\right)\right], \tag{A32}$$

$$H_{19j} = (t_j^2 - t_{j-1}^2)\log[h_j], \quad H_{20j} = (t_j - t_{j-1})\log[h_j], \tag{A33}$$

$$H_{20j} = (t_j - t_{j-1})\log[h_j], \quad H_{21j} = [a_j - a_{j-1} + y(k_j - k_{j-1})]\log[h_j], \tag{A34}$$

$$M^j_{1m} = \frac{\sqrt{\mu_m^2 + r^j_{[2m]}}}{1+k^2_{[2m]}}, \quad M^j_{2m} = k_{[2m]} M^j_{1m}, \quad M_{3m} = \frac{\mu_m - k_{[2m]}\vartheta_{[2m]}}{\left(1+k^2_{[2m]}\right)[\mu_m + \vartheta^2_{[2m]}]}, \tag{A35}$$

$$M^j_{4m} = \frac{\left(\mu_m - k_{[2m]}\vartheta_{(m)}\right)\sqrt{\mu_m^2 + r^j_{(m)}}}{(1+k^2)\left[\mu_m^2 + \vartheta^2_{(m)}\right]}, \quad M^j_{5m} = \frac{k^2_{[2m]} s_j z(\alpha_m - k^2_{[2m]}\beta_{(m)})}{\left(1+k^2_{[2m]}\right)\left(\alpha_m^2 + k^2_{[2m]}\beta^2_{(m)}\right)}, \tag{A36}$$

$$M^j_{6m} = \frac{k_{[2m]}\left(\alpha_m - k^2_{[2m]}\beta_{(m)}\right)\sqrt{\alpha_m^2 + k^2_{[2m]}\left(\beta^2_{(m)} + s_j^2 z^2\right)}}{\left(1+k^2_{[2m]}\right)\left(\alpha_m^2 + k^2_{[2m]}\beta^2_{(m)}\right)}, \tag{A37}$$

$$M^j_{7m} = \frac{\left(k_{[2m]}\mu_m + \vartheta_{(m)}\right)s_j z}{\left(1+k^2_{[2m]}\right)\left[\mu_m^2 + \vartheta^2_{(m)}\right]}, \quad M^j_{8m} = \frac{\left(k_{[2m]}\mu_m + \vartheta_{(m)}\right)\sqrt{\mu_m^2 + r^j_{(m)}}}{\left(1+k^2_{[2m]}\right)\left[\mu_m^2 + \vartheta^2_{(m)}\right]}, \tag{A38}$$

$$M^j_{9m} = \sqrt{(s_j g_m)^2 + h_{[2m]}}, \quad M_{10m} = \frac{g_m^2 \beta_{[2m]} + 2k_{[2m]} x^2 \gamma_{(m)} + k^2_{[2m]} x^2 (y + y_{(m)})}{h_{(m)}}, \tag{A39}$$

$$M^j_{11m} = \frac{\left[k_{[2m]}(2x^2 + 2y^2 - 3yy_{(m)} + y^2_{(m)}) + \beta_{(m)}\gamma_{(m)}\right]}{h_{(m)}} M^j_{9m}, \tag{A40}$$

$$M_{12m} = \frac{g^2_{2[2m]-1} - g^2_{2[2m]} + (k^2_{[2m]} - k^2_{[2(m+2)]})h_{[2m]}}{h_{[2m]}}, \tag{A41}$$

$$M_{13j} = \begin{cases} \frac{3(k_j\gamma_{j-1} - k_{j-1}\gamma_j) + (k_j^2 - k_{j-1}^2)(y+2y_j)}{h_j^2}, & (1 \leqslant j \leqslant 3) \\ \frac{\beta_{j-3} q^2_{j-4} - \beta_{j-4} q^2_{j-3} + x^2[(k^2_{j-3} - k^2_{j-4})(y+y_{j-3}) + 2(a_{j-3}-1)k_{j-3} - 2(a_{j-4}-1)k_{j-4}]}{h^2_{j-3}}, & (4 \leqslant j \leqslant 6) \end{cases} \tag{A42}$$

$$M^j_{14m} = \frac{x\left[k_{[2m]}(x^2 + y^2 - 3yy_{(m)} + 2y^2_{(m)}) - \beta_{(m)}\gamma_{(m)}\right]}{h^2_{(m)}} M^j_{8m}, \tag{A43}$$

$$M^j_{15m} = \frac{\left[\left(\gamma_{(m)} - k_{[2m]}(2y - 3y_{(m)})\right)h_{(m)} - 2x^2 g_m\right]}{h^2_{(m)}} M^j_{8m}, \tag{A44}$$

$$M_{16j} = \begin{cases} \frac{u_j + (t_j^2 - t_{j-1}^2)(x^2 + \beta_j)}{h_j^2}, & (j \leqslant 3) \\ \frac{2x^2\left[u_j + 2(\gamma_{j-3} - \gamma_{j-4})\beta_{j-3} + (t_{j-3}^2 - t_{j-4}^2)(5x^2 + 3y^2 - 4yy_{j-3})\right]}{h_{j-3}}, & (4 \leqslant j \leqslant 6) \end{cases} \tag{A45}$$

$$M_{17j} = \frac{(a_j - a_{j-1})\beta_j + (k_j - k_{j-1})(x^2 + y^2 - yy_j)}{h_j}, \quad M_{18j} = \frac{(k_j - k_{j-1})y_j + a_j - a_{j-1}}{h_j}, \tag{A46}$$

$$L_{1m}^j = -i[x + (-1)^m i s_j z] \log\left[\frac{\lambda_{m+2}^j\left(\mu_{2[2m]-1} + (-1)^{m+1} i s_j z \lambda_m^j/\theta_m^j + \sqrt{\mu_{2[2m]-1}^2 + r_{[2m]}^j}\right)}{\lambda_m^j\left(\mu_{2[2m]} + (-1)^{m+1} i s_j z \lambda_{m+2}^j/\theta_m^j + \sqrt{\mu_{2[2m]}^2 + r_{[2(m+2)]}^j}\right)}\right], \tag{A47}$$

$$L_{2m}^j = \frac{\nu_{[2m]}}{\gamma_{[2m]}} p_m^j, \tag{A48}$$

$$L_{3m}^j = [x + (-1)^m i s_j z] \log\left[\frac{(\theta_{2[2m]}^j)^2\left[\mu_{2[2m]-1}\theta_{2[2m]-1}^j + (-1)^{m+1} i s_j z \lambda_m^j + \theta_{2[2m]-1}^j\sqrt{\mu_{2[2m]-1}^2 + r_{[2m]}^j}\right]}{(\theta_{2[2m]-1}^j)^2\left[\mu_{2[2m]}\theta_{2[2m]}^j + (-1)^{m+1} i s_j z \lambda_m^j + \theta_{2[2m]}^j\sqrt{\mu_{2[2m]}^2 + r_{[2(m+2)]}^j}\right]}\right], \tag{A49}$$

$$L_{4m}^j = i \log\left[\frac{(\theta_{2[2m]}^j)^2\left[\mu_{2[2m]-1}\theta_{2[2m]-1}^j + s_j^2 z^2 + \nu_{2[2m]-1}\sqrt{\mu_{2[2m]-1}^2 + r_{[2m]}^j}\right]}{(\theta_{2[2m]-1}^j)^2\left[\mu_{2[2m]}\theta_{2[2m]}^j + s_j^2 z^2 + \nu_{2[2m]}\sqrt{\mu_{2[2m]}^2 + r_{[2(m+2)]}^j}\right]}\right], \tag{A50}$$

$$L_{5m}^j = \frac{1}{\gamma_{[2m]}} p_m^j, \tag{A51}$$

$$L_{6m}^j = \log\left[\frac{\left(\mu_{2[2m]-1}(\theta_m^j)^2 + (-1)^{m+1} i s_j z \theta_m^j \lambda_{2[2m]-1} + \sqrt{\mu_{2[2m]-1}^2 + r_{[2m]}^j}\right)}{\left(\mu_{2[2m]}(\theta_m^j)^2 + (-1)^{m+1} i s_j z \theta_m^j \lambda_{2[2m]} + \sqrt{\mu_{2[2m]}^2 + r_{[2(m+2)]}^j}\right)}\right], \tag{A52}$$

$$L_{8m}^j = \frac{\left(\nu_{[2m]}^2 - \gamma_{[2m]}^2 x^2 - i\gamma_{[2m]} s_j^2 z^2\right)}{\gamma_{[2m]}^2 s_j^2 z^2} p_m^j, \tag{A53}$$

$$L_{7m}^j = \frac{(x_{[2m]} - 2x)x_{[2m]}}{s_j^2 z^2} \log\left[\frac{\left[\vartheta_{[2m]}\left(\vartheta_{[2m]} + i\mu_{2[2m]-1}\right) + s_j^2 z^2 + s_j z\sqrt{\mu_{2[2m]-1}^2 + r_{[2m]}^j}\right]}{\left[\vartheta_{[2m]}\left(\vartheta_{[2m]} - i\mu_{2[2m]}\right) + s_j^2 z^2 + s_j z\sqrt{\mu_{2[2m]}^2 + r_{[2(m+2)]}^j}\right]}\right], \tag{A54}$$

$$L_{9m}^j = \frac{2k_{[2m]}\rho_m s_j^2 - y}{s_j} f_m^j, \quad L_{10m}^j = \frac{2k_{[2m]}\rho_m s_j^2 + y + 2i(-1)^m x}{s_j} f_m^j, \tag{A55}$$

$$L_{11m}^j = \frac{i(2s_j^2 k_{[2m]}\rho_m + (-1)^m i x)}{s_j} f_m^j, \quad L_{12m}^j = i s_j \rho_m f_m^j, \quad L_{13m}^j = i s_j t_{[2m]}^2 f_m^j, \quad L_{14m}^j = i f_m^j, \tag{A56}$$

$$L_{15m}^j = \frac{i[1 + (s_j k_{[2m]})^2]}{s_j} f_m^j, \quad L_{16m}^j = \frac{1}{s_j} f_m^j, \quad L_{17m}^j = \frac{[1 + 2(s_j k_{[2m]})^2]}{s_j} f_m^j, \tag{A57}$$

$$L_{18m}^j = k_{[2m]} f_m^j, \quad L_{19m}^j = \rho_m f_m^j, \quad L_{20m}^j = [y + (-1)^m i x] f_m^j. \tag{A58}$$

References

[1] S.L. Crouch, Solution of plane elasticity problems by the displacement discontinuity method, Int. J. Numer. Methods Eng. 10 (1976) 301–343.
[2] Y.C. Pan, T.W. Chou, Point force solution for an infinite transversely isotropic solid, ASME J. Appl. Mech. 43 (1976) 608–612.
[3] D.J. Bacon, D.M. Barnett, R.O. Scattergood, Anisotropic continuum theory of lattice defects, Prog. Mater. Sci. 23 (1978) 51–262.
[4] T. Mura, Micromechanics of Defects in Solids, second ed., Martinus Nijhoff, 1987.
[5] T.C.T. Ting, Anisotropic Elasticity: Theory and Applications, Oxford University Press, New York, 1996.
[6] M. Kachanov, B. Shafiro, I. Tsukrov, Handbook of Elasticity Solutions, Kluwer Academic Publishers, Boston, 2003.
[7] E. Pan, A BEM analysis of fracture mechanics in 2D anisotropic piezoelectric solids, Eng. Anal. Bound. Elem. 23 (1999) 67–76.

[8] H.J. Ding, J. Liang, B. Chen, The united point force solution for both isotropic and transversely isotropic media, Commun. Numer. Methods Eng. 13 (1997) 95–102.
[9] M.L. Dunn, H.A. Wienecke, Half-space Green's functions for transversely isotropic piezoelectric solids, J. Appl. Mech. 66 (1999) 675–679.
[10] W.Q. Chen, T. Shioya, H.J. Ding, The elasto-electric field for a rigid conical punch on a transversely isotropic piezoelectric half-space, J. Appl. Mech. 66 (1999) 764–771.
[11] E. Pan, F. Tonon, Three-dimensional Green's functions in anisotropic piezoelectric solids, Int. J. Solids Struct. 37 (2000) 943–958.
[12] C.F. Gao, M.Z. Wang, Green's functions of an interfacial crack between two dissimilar piezoelectric media, Int. J. Solids Struct. 38 (2001) 5323–5334.
[13] H.J. Ding, W.Q. Chen, A.M. Jiang, Green's functions and boundary element method for transversely isotropic piezoelectric materials, Eng. Anal. Bound. Elem. 28 (2004) 975–987.
[14] M.H. Zhao, Y.P. Shen, Y.J. Liu, G.L. Liu, Isolated crack in three-dimensional piezoelectric solid: Part I: solution by Hankel transform, Theor. Appl. Fract. Mech. 26 (1997) 129–139.
[15] C.Y. Fan, M.H. Zhao, Y.H. Zhou, Numerical solution of polarization saturation/dielectric breakdown model in 2D finite piezoelectric media, J. Mech. Phys. Solids 57 (2009) 1527–1544.
[16] M.H. Zhao, G.T. Xu, C.Y. Fan, Hybrid extended displacement discontinuity-charge simulation method for analysis of cracks in 2D piezoelectric media, Eng. Anal. Bound. Elem. 33 (2009) 592–600.
[17] M.H. Zhao, C.Y. Fan, T. Liu, F. Yang, Extended displacement discontinuity Green's functions for three dimensional transversely isotropic magneto-electro-elastic media and applications, Eng. Anal. Bound. Elem. 31 (2007) 547–558.
[18] M.H. Zhao, R.L. Zhang, C.Y. Fan, E. Pan, Three-dimensional extended displacement discontinuity method for vertical cracks in transversely isotropic piezoelectric media, Eng. Anal. Bound. Elem. 36 (2012) 1406–1415.
[19] O.J. Svec, G.M.L. Gladwell, An explicit Boussinesq solution for a polynomial distribution of pressure over a triangular region, J. Elast. 1 (1971) 167–170.
[20] J.J. Kalker, Y. van Randen, A minimum principle for frictionless elastic contact with application to non-hertzian half-space contact problems, J. Eng. Math. 6 (1972) 193–206.
[21] J.R. Dydo, H.R. Busby, Elasticity solutions for constant and linearly varying load applied to a rectangular surface patch on the elastic half-space, J. Elast. 38 (1995) 153–163.
[22] C.D. Wang, J.J. Liao, Elastic solutions for a transversely isotropic half-space subjected to arbitrarily shaped loads using triangulating technique, Int. J. Geomech. 1 (2001) 193–224.
[23] J.S. Li, E.J. Berger, A Boussinesq–Cerruti solution set for constant and linear distribution of normal and tangential load over a triangular area, J. Elast. 63 (2001) 137–151.
[24] H.T. Xiao, Z.Q. Yue, Elastic fields in two joined transversely isotropic media of infinite extent due to rectangular load, Int. J. Numer. Anal. Methods Geomech. 10 (2011) 1002.
[25] H.J. Ding, W.Q. Chen, L. Zhang, Elasticity of Transversely Isotropic Materials, Springer, Netherlands, 2006.
[26] M.H. Zhao, Y.P. Shen, Y.J. Liu, G.L. Liu, Crack analysis in semi-infinite transversely isotropic piezoelectric solid. I. Green's functions, Theor. Appl. Fract. Mech. 32 (1999) 223–232.
[27] H.M. Wang, E. Pan, A. Sangghaleh, R. Wang, X. Han, Circular loadings on the surface of an anisotropic and magnetoelectroelastic half-space, Smart Mater. Struct. 21 (2012) 075003.